Journal of Solid State Chemistry 182 (2009) 3353–3357

Contents lists available at ScienceDirect

Journal of Solid State Chemistry

journal homepage: www.elsevier.com/locate/jssc

Preparation and properties of antiperovskite-type nitrides: $InNNi_3$ and $InNCo_3$

W.H. Cao [a,b], B. He [a,c], C.Z. Liao [a,b], L.H. Yang [a], L.M. Zeng [b], C. Dong [a,*]

[a] National Laboratory for Superconductivity, Institute of Physics and Beijing National Laboratory for Condensed Matter Physics, Chinese Academy of Science, Beijing 100190, China
[b] College of Physical Science and Technology, Guangxi University, Nanning 530004, China
[c] Luzhou Medical College, Luzhou, Sichuan 646000, China

ARTICLE INFO

Article history:
Received 5 May 2009
Received in revised form
26 September 2009
Accepted 2 October 2009
Available online 8 October 2009

Keywords:
Nitride
Antiperovskite
Nitrogen content
Spin-glass-like

ABSTRACT

Two antiperovskite-type ternary nitrides of $InNM_3$ (M=Ni, Co) have been synthesized from In_2O_3 and Ni or Co powders under NH_3 atmosphere at 600 °C. $InNCo_3$ is a new ternary nitride whereas $InNNi_3$ was previously reported as $InN_{0.5}Ni_3$ with different nitrogen content. The lattice parameters refined by Rietveld method are 3.8445(1) Å for $InNNi_3$ and 3.8541(7) Å for $InNCo_3$, respectively. Both nitrides show metallic behaviors and below 70 K the T^2 temperature dependence of resistivity was observed indicative of a Fermi liquid behavior. The temperature dependence of the field-cooling (FC) and zero-field-cooling (ZFC) magnetization and time decay of thermoremanent magnetization indicate the spin-glass-like behavior in $InNM_3$ (M=Ni, Co). The freezing temperatures for this behavior, T_f, are about 300 K for $InNNi_3$ and 10 K for $InNCo_3$, respectively.

1. Introduction

Since the superconductivity of $MgCNi_3$ with T_c=8 K has been discovered [1], extensive studies on antiperovskite materials were performed in the search for new superconductors. Among the investigated antiperovskite carbides i.e., $ACNi_3$ (A=Zn, Al, Ga, In, Cd, and so on), only $CdCNi_3$ is a superconductor with T_c=3.4 K [2]. $ZnCNi_3$ was reported to be a Pauli paramagnetic (PM) metal without onset of superconductivity down to 2 K [3]. $In_{0.95}CNi_3$ behaves as a ferromagnetic metal below the Curie temperature (577 K) [4]. In addition to the antiperovskite carbides, many antiperovskite nitrides have been studied. The $MNFe_3$ (M=Fe, Mn, Au, Ag, Sn, Pd, Ni, Pt) compounds, for example, exhibit interesting Invar-like behavior [5–13]. Mn-based antiperovskite nitrides $ANMn_3$ (A=Cu, Zn, Ga, Ge, etc.) show large negative thermal expansion triggered by an antiferromagnetic or ferromagnetic transition [14,15]. These facts indicate that fascinating physical properties might be expected in new 3d-transition metal-based antiperovskite nitrides.

Very recently, a new superconductor ZnN_yNi_3 with $T_c \sim 3$ K was found [16], which is the first antiperovskite nitride superconducting material. InN_yNi_3 has one more valence electron than ZnN_yNi_3 and might have different properties from ZnN_yNi_3. A fully ordered compound $InN_{0.5}Ni_3$ (ICDD-PDF: 28-0700) with lattice parameter a=3.84 Å was reported in 1976, but until now there has been no detailed report on the method for synthesizing this compound. $InNCo_3$ with the same structure was predicted in reference [17] and its experimental verification is absent so far. This work is an effort to find a suitable route to prepare $InNNi_3$ and $InNCo_3$ and study their physical properties.

2. Experimental

2.1. Sample preparation

We prepared a series of InN_yM_3 (M=Ni, Co) samples by solid–gas reactions of In_2O_3 (> 99%) and metal powders (Ni (99.5%), Co (99.7%)) with NH_3 (99.9% purity) at ambient pressure. The starting materials were weighed with the nominal composition of In:M=1:3 and were thoroughly ground, and then put into alumina boats. The mixtures were heated in a tube furnace at 600–650 °C for 10 h under static NH_3 atmosphere and subsequently furnace cooled to room temperature. During the heating process, fresh NH_3 gas was refilled five times to remove the H_2O vapor produced in the reaction. The obtained intermediate products consisted of loose coarse powder and corresponding X-ray diffraction (XRD) analyses indicated that each is a single-phased antiperovskites. To improve consistency in the resistivity and magnetic measurements, the intermediate products were then reground thoroughly, pressed into pellets and sintered for another 10 h under the same reaction conditions. In addition, compounds $InNM_3$ (M=Ni, Co)

* Corresponding author.
E-mail address: chengdon@aphy.iphy.ac.cn (C. Dong).

0022-4596/$ - see front matter © 2009 Elsevier Inc. All rights reserved.
doi:10.1016/j.jssc.2009.10.002

can also be synthesized by using the corresponding transition metal oxide as a precursor instead of metal powders.

2.2. Powder XRD measurements and elemental analyses

The powder X-ray diffraction data were collected on a MXP18A-HF diffractometer with Cu$K\alpha$ radiation at room temperature. The 2θ scan range was from 20° to 120° with a step size of 0.02° and a counting time of 3 s. The XRD data were analyzed by the Rietveld technique, using the program RIETAN2000 [18]. An energy dispersive X-ray (EDX) spectrometer (on a scanning electron microscope XL30 S-FEG) was used to analyze the sample compositions and a Vario MICRO CUBE (Germany) elemental analyzer was employed to determine the nitrogen content.

2.3. Physical property measurements

The temperature dependence of electrical resistivity was measured using the four-probe method in the temperature range of 5–300 K. The relationships of magnetization versus temperature were obtained by using a SQUID (Quantum Design PPMS) magnetometer in the temperature range of 2–300 K. Data were collected under both zero-field-cooled (ZFC) and field-cooled (FC) conditions in an applied field of 20 Oe.

3. Results and discussion

3.1. Nitrogen content and crystal structure of InN_yM_3

Figs. 1(a) and (b) show the EDX spectra of samples InN_yM_3 (M=Ni, Co). According to the EDX analysis, the atomic ratios (atomic %) of In:Ni and In:Co in samples InN_yNi_3 and InN_yCo_3 are 1.0:2.86 and 1.0:2.81, respectively, and they are consistent with the nominal ratio (1:3) within the experimental error around 7%. In addition, no impurity phase was found in the powder XRD patterns, which indicates the In:M ratios are in agreement with the nominal ones.

Fig. 2 shows the powder XRD patterns for InN_yM_3 (M=Ni, Co). It is found that all diffraction patterns can be well indexed to the antiperovskite-type structure with space group $Pm3m$. Using the antiperovskite structure as a starting model, the lattice parameters and nitrogen content y for both nitrides were refined by Rietveld method. From the analysis, we obtained the lattice parameter a=3.854 Å for InN_yCo_3 and a=3.844 Å for InN_yNi_3. The elemental analysis showed that the weight percentages of nitrogen are 3.7 and 4.7% for InN_yNi_3 and InN_yCo_3, corresponding to the values of $y\sim0.8$ and 1.0, respectively. According to the results, we first tried to fix the nitrogen occupancy with 0.8 for InN_yNi_3 in the Rietveld refinement, and found that the isotropic thermal parameter of the nitrogen atom (B_N) turns out to be an irrational negative value. Then, we tried to fix the B_N parameter with a reasonable value, and found that the nitrogen occupancy increased to 0.97, indicating an almost full occupation of the nitrogen atom. Based on the above analysis, we inferred that the nitrogen content in InN_yNi_3 obtained from elemental analysis may deviate from the real value due to the instability and inhomogeneity of InN_yNi_3. For the final refinement, the occupancy factor of the N atom was fixed to 1.0 and reliability factors R_{wp}=0.095, R_P=0.062 were obtained. As for InN_yCo_3, the nitrogen contents of y obtained from the elemental analysis and from the Rietveld analysis are consistent with each other, so the value of y in InN_yCo_3 was decided to be 1.0. Table 1 lists the final R factors and the refined structural parameters. Fig. 2 shows the Rietveld refinement patterns for $InNNi_3$ (a) and $InNCo_3$ (b).

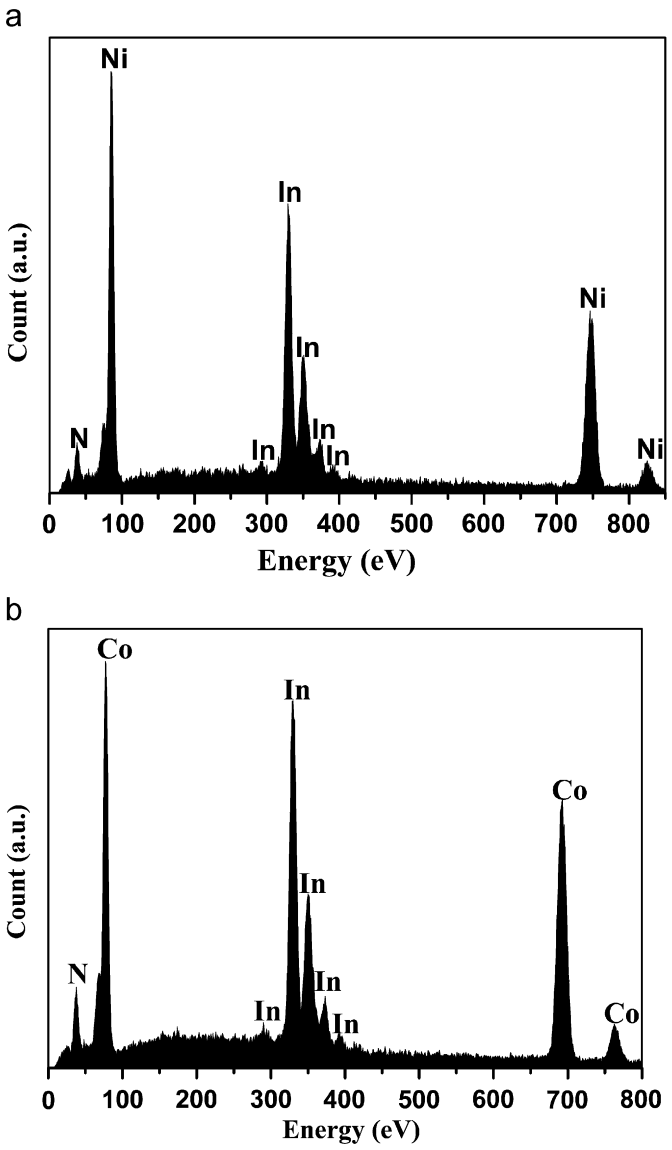

Fig. 1. (a) EDX spectrum of $InNNi_3$. (b) EDX spectrum of $InNCo_3$.

3.2. Electronic and magnetic properties of $InNM_3$

The temperature dependence of the resistivity for $InNNi_3$ and $InNCo_3$ are shown in Figs. 3 and 4, respectively. Both compounds exhibit metallic behaviors over the whole temperature range measured and no superconductivity is found down to 5 K. As can be seen in the inset of Figs. 3 and 4, below 70 K the resistivity can be fitted with the equation

$$\rho(T)=\rho_0+AT^2 \quad (1)$$

which is suggestive of a Fermi liquid behavior. The residual resistivity ρ_0 and parameter A are found to be 39.06(4) μΩ cm and 0.012 μΩ cm/K^2 for $InNCo_3$ and 407.13(6) μΩ cm and 0.027 μΩ cm/K^2 for $InNNi_3$, respectively. At high temperatures (70–300 K) the resistivity for $InNNi_3$ shows a linear behavior, which is attributed to electron–phonon scattering.

Fig. 5 shows the temperature dependence of magnetization for $InNNi_3$ in zero-field-cooled (ZFC) and field-cooled (FC) at a magnetic field of 20 Oe. Both the FC and ZFC magnetization

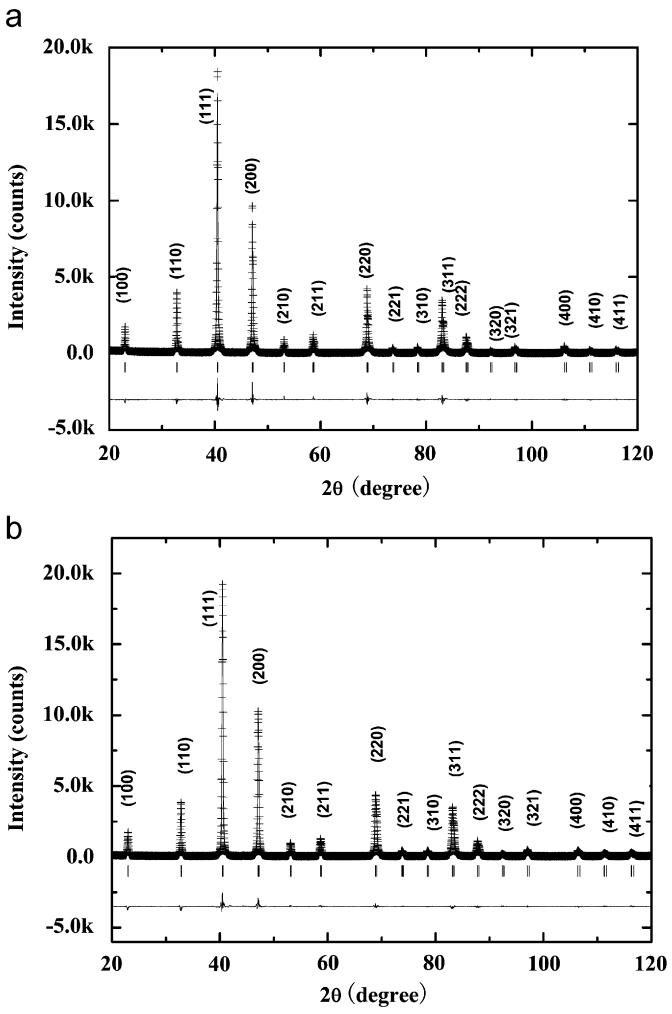

Fig. 2. The Rietveld refinement patterns for $InNNi_3$ (a) and $InNCo_3$ (b). The lines with plus marks (+) represent the observed diffraction patterns, the solid lines represent the calculated patterns, and the curves at the bottom of each figure represent the difference between the observed and calculated patterns. The short vertical lines mark the positions of allowed reflections.

Table 1
Refined structural parameters for $InNNi_3$ (a) and $InNCo_3$ (b).

Atom	Site	x	y	z	B (Å^2)	Occupancy
In	1a	0	0	0	1.1	1.0
N	1b	0.5	0.5	0.5	1.8	1.0
Ni	3c	0	0.5	0.5	1.1	1.0
R_p=6.19%, R_{wp}=9.51%, R_{ex}=6.61%, a=3.8445(1) Å						
In	1a	0	0	0	1.3	1.0
N	1b	0.5	0.5	0.5	1.1	1.0
Ni	3c	0	0.5	0.5	1.4	1.0
R_p=7.89%, R_{wp}=10.58%, R_{ex}=6.98%, a=3.8541(7) Å						

decrease monotonically at low T, indicating a tendency of paramagnetic behavior. But with increasing temperature, the ZFC magnetization increase and the FC decrease and the two trendlines meet each other at about 300 K. The differences between FC and ZFC magnetization may be explained by spin glasses [19–21] or inhomogeneous cluster systems [22–25]. Therefore we also measured the time dependence of remanent magnetization at different temperature to further understand the actual behavior in this system. A magnetic field of 20 Oe was

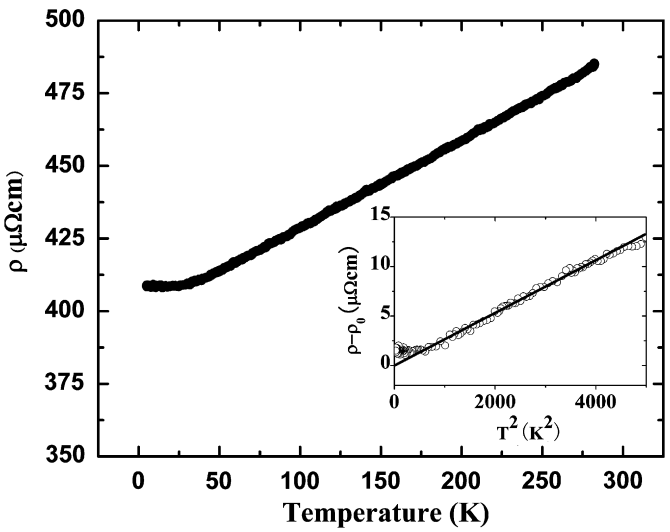

Fig. 3. Temperature-dependent resistivity of $InNNi_3$. Inset: linear fitting of $\rho(T)-\rho_0$ vs T^2 below 70 K.

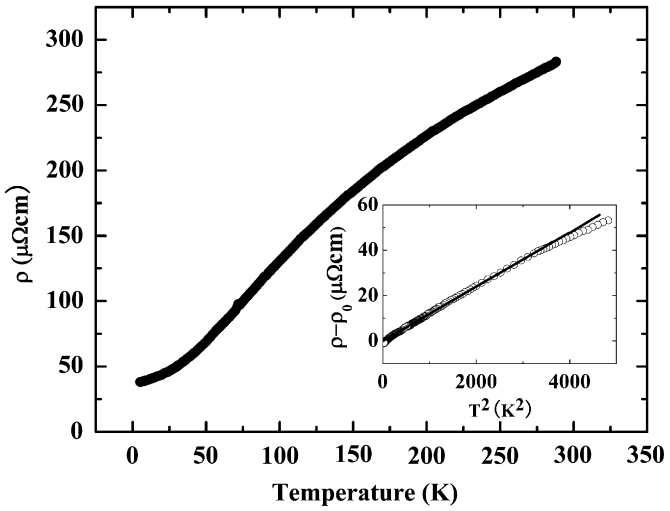

Fig. 4. Temperature-dependent resistivity of $InNCo_3$. Inset: linear fitting of $\rho(T)-\rho_0$ vs T^2 below 70 K.

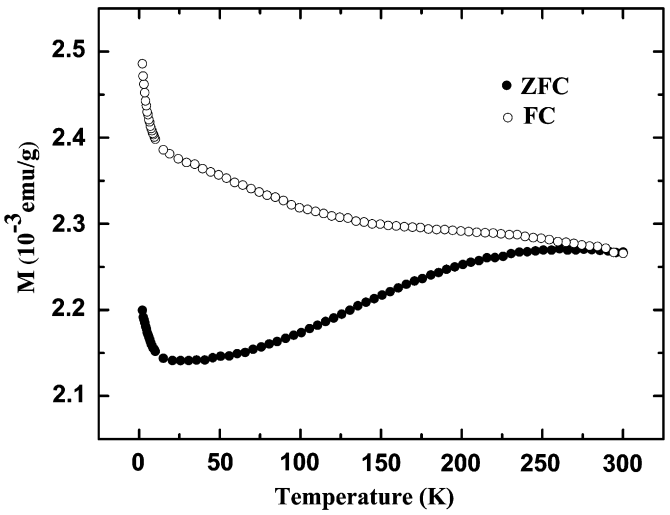

Fig. 5. Temperature dependence of the zero-field-cooling (ZFC) and field-cooling (FC) dc magnetization curves in an applied magnetic field of 20 Oe for $InNNi_3$.

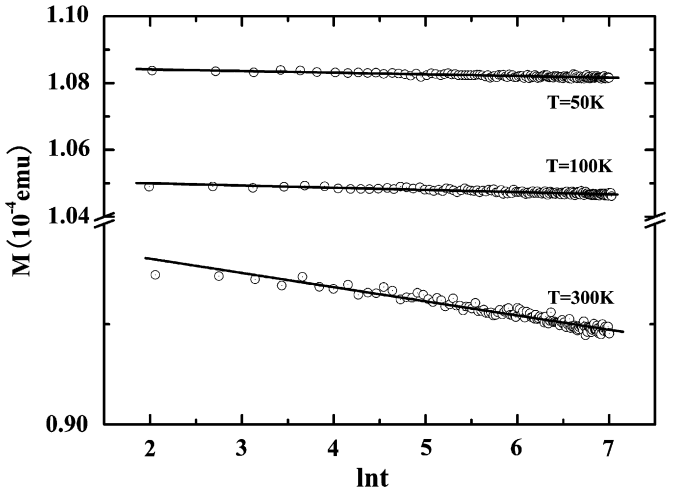

Fig. 6. Time dependence of remanent magnetization at 50, 100 and 300 K for $InNNi_3$. The solid curves exhibit the linear fitting with Eq. (2).

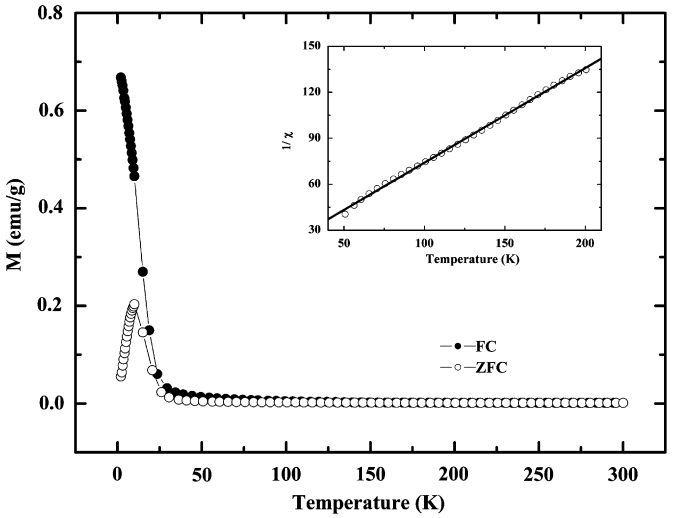

Fig. 7. Temperature dependence of the zero-field-cooling (ZFC) and field-cooling (FC) dc magnetization curves in an applied magnetic field of 20 Oe for $InNCo_3$. The inset shows inverse susceptibility curve with the fitting of Curie–Weiss law in the temperature range 50–200 K.

Table 2
Values of the parameters M_0 and S of Eq. (2) for sample $InNNi_3$.

Temperature (K)	M_0 (10^{-5} emu)	S (10^{-7} emu)
50	10.851	0.4967
100	10.513	0.6585
300	9.1934	1.4136

applied at 300 K and then the sample was cooled down to the measuring temperature. The magnetic field was set to zero after the temperature was stabilized, and $M(t)$ measurements were started and continued up to 10,000 s. As is shown in Fig. 6, the plotted curve can be fitted in the form of equation [26,27]:

$$M(t) = M_0 - S\ln(t) \quad (2)$$

Here S is called the "magnetic viscosity" and M_0 is a constant at a given applied field. The values of M_0 and S are given in Table 2. M_0 decreases with increasing temperature, while the coefficient S increases linearly with increasing temperature prior to reaching a freezing temperature for the behavior. This is typical of spin-glass-like (SGL) systems [28,29], which suggests $InNNi_3$ exhibits SGL behavior.

Fig. 7 displays the FC and ZFC magnetization curves for $InNCo_3$. At high temperature, the ZFC and FC are well consistent with each other. The ZFC curve between 50 and 200 K could be fitted to a Curie–Weiss law:

$$\chi = C/(T - \theta_p) \quad (3)$$

where C is the Curie constant and θ_p is the paramagnetic Curie temperature. The fitting result based on Eq. (3) gives the values of parameters, C=1.62 K, θ_p=−20.10 K, respectively. The effective magnetic moment per Co atom, μ_{eff} is estimated as 3.44 μ_B. The negative value of θ_p indicates antiferromagnetic (AFM) interactions in the sample. The fitted curve is shown in the inset of Fig. 7. However, at low temperature, a bifurcation between the ZFC and FC curve at the freezing temperature T_f=10 K is observed. Such a bifurcation could be an indication of spin glass behavior, which is similar to that reported in compounds $Li_{2.5}Co_{0.5}N$, $LaNi_{1/2}Rh_{1/2}O_3$ and $Y_{0.5}Sr_{0.5}MnO_3$ [30–32].

The SGL behavior observed in $InNNi_3$ and $InNCo_3$ might be attributed to competition between ferromagnetic and antiferromagnetic interactions. Nevertheless, the magnetic properties of $InNNi_3$ and $InNCo_3$ are rather complex and additional studies are needed to elucidate the mechanism for their SGL behaviors. Recently, a similar behavior has been observed in an antiperovskite compound $GaNMn_3$ by Song et al. [33]. A variety of magnetic behavior has been reported for $GaNMn_3$ in the prior literatures [34–39]. Song et al. attribute these differences to the differences in the various synthesis routes employed for this compound and the resulting variation in compositions. We suspect a similar variation in magnetic behaviors may also be found in the $InNM_3$ (M=Ni, Co) compounds. The compositional sensitivity of the magnetic behavior in these nitrides should be studied in greater detail.

4. Conclusion

In summary, two ternary nitrides $InNM_3$ (M=Ni, Co) were synthesized by solid–gas reactions of metal powders with NH_3. Both $InNNi_3$ and $InNCo_3$ adopt the antiperovskite crystal structure, and their lattice parameters are 3.854 and 3.844 Å, respectively. These two compounds show metallic behavior in temperature dependence of the resistivity from 5 to 300 K, and exhibit a Fermi liquid behavior below 70 K. Measurements of magnetization indicates that they have spin-glass-like properties. $InNNi_3$ and $InNCo_3$ are two new members of the larger category of antiperovskite nitrides and the synthesis route employed in this work may be used to prepare other nitride-containing antiperovskites. The synthesis and systematic study of these types of antiperovskites are important in identifying and understanding new structure-property relationships. Studies on new nitride-containing antiperovskites by substituting In and Ni with other metals are well under way in our laboratory.

Acknowledgments

This work was supported by the National Natural Science Foundation of China (Nos. 20271052 and 20571083) and MOST 973 project (No. 2006CB601004).

References

[1] T. He, Q. Huang, A.P. Ramirez, Y. Wang, K.A. Regan, N. Rogado, M.A. Hayward, M.K. Haas, J.S. Slusky, K. Inumara, H.W. Zandbergen, N.P. Ong, R.J. Cava, Nature 411 (2001) 54.
[2] M. Uehara, T. Amano, S. Takano, T. Kôri, T. Yamazaki, Y. Kimishima, Physica C 440 (2006) 6.
[3] M.S. Park, J. Giim, S.H. Park, Y.W. Lee, S.I. Lee, E.J. Choi, Supercond. Sci. Technol. 17 (2004) 274.
[4] P. Tong, Y.P. Sun, X.B. Zhu, W.H. Song, Solid State Commun. 141 (2007) 336.
[5] S.F. Matar, P. Mohn, G. Demazeau, B. Siberchicot, J. Phys. 49 (1988) 1761 (Paris).
[6] S.F. Matar, G. Demazeau, B. Siberchicot, IEEE Trans. Magn. 26 (1990) 60.
[7] C. Cordier-Robert, J. Foct, Eur. J. Solid State Inorg. Chem. 29 (1992) 39.
[8] P. Mohn, K. Schwarz, S.F. Matar, G. Demazeau, Phys. Rev. B 45 (1992) 4000.
[9] C.A. Kuhnen, R.S. de Figueiredo, V. Drago, E.Z. da Silva, J. Magn. Magn. Mater. 111 (1992) 95.
[10] C.A. Kuhnen, A.V. dos Santos, Solid State Commun. 85 (1993) 273.
[11] C.A. Kuhnen, A.V. dos Santos, J. Magn. Magn. Mater. 130 (1994) 353.
[12] S. Suzuki, H. Sakamoto, J. Minegismi, V. Omote, IEEE Trans. Magn. 17 (1981) 3017.
[13] S.F. Matar, G. Demazeau, P. Hagenmuller, J.G.M. Armitage, P.C. Riedi, Eur. J. Solid State Inorg. Chem. 26 (1989) 517.
[14] D. Fruchart, E.F. Bertaut, J. Phys. Soc. Jpn. 44 (1978) 781.
[15] K. Takenaka, H. Takagi, Appl. Phys. Lett. 87 (2005) 261902.
[16] M. Uehara, A. Uehara, K. Kozawa, Y. Kimishima, J. Phys. Soc. Jpn. 78 (2009) 033702.
[17] B.V. Beznosikov, J. Struct. Chem. 44 (2003) 885.
[18] F. Izumi, T. Ikeda, Mater. Sci. Forum 189 (2000) 321.
[19] J.A. Mydosh, Spin Glasses: An Experimental Introduction, Taylor and Francis, London, 1993.
[20] S. Chikuzami, Physics of Ferromagnetism, Clarendon, Oxford, 1997.
[21] G. Williams, in: R.A. Hein, T.L. Franca villa, D.H. Liebenberg (Eds.), Magnetic Susceptibility and Other Spin Systems, Plenum, New York, 1991, p. 475.
[22] J.L. Tholance, in: R.A. Hein, T.L. Franca villa, D.H. Liebenberg (Eds.), Magnetic Susceptibility and Other Spin Systems, Plenum, New York, 1991, p. 503.
[23] J.L. Dormann, R. Charkaoui, L. Spinu, M. Nogues, F. Lucari, F. Dorazio, D. Fiorani, A. Garcia, E. Tronc, J.P. Jolivet, J. Magn. Magn. Mater. 187 (1985) L139.
[24] H. Maniya, I. Nakatani, T. Furubayashi, Phys. Rev. Lett. 80 (1998) 177.
[25] J.A. Detoro, M.A. Lopez de la Torre, J.M. Riveiro, R. Saez Puche, A. Gomez-Herrero, L.C. Otero-Diaz, Phys. Rev. B 60 (1999) 12918.
[26] R. Street, J.C. Woolley, Proc. Phys. Soc. Section A 62 (1949) 562.
[27] C.N. Guy, J. Phys. F Met. Phys. 8 (1978) 1309.
[28] S.D. Tiwari, K.P. Rajeev, Phys. Rev. B 72 (2005) 104433.
[29] R.S. Patela, A.K. Majumdar, A.K. Nigam, J. Magn. Magn. Mater. 309 (2007) 256.
[30] C. Schinzer, J. Alloys. Compd. 288 (1999) 65.
[31] S. Chatterjee, A.K. Nigam, Phys. Rev. B 66 (2002) 104403.
[32] D.L. Liu, F. Du, Y.J. Wei, Mater. Lett. 63 (2009) 133.
[33] B. Song, J.K. Jian, H.Q. Bao, M. Lei, H. Li, G. Wang, Y.P. Xu, X.L. Chen, Appl. Phys. Lett. 92 (2008) 192511.
[34] E.F. Bertaut, D. Fruchart, Solid State Commun. 6 (1968) 251.
[35] J.P. Bouchard, Ann. Chim. 3 (1968) 81 (Paris).
[36] K.H. Kim, K.J. Lee, D.J. Kim, Y.E. Ihm, D. Djayaprawira, M. Takahashi, C.S. Kim, C.G. Kim, S.H. Yoo, Appl. Phys. Lett. 82 (2003) 1775.
[37] K.H. Kim, K.J. Lee, H.S. Kang, F.C. Yu, J.A. Kim, D.J. Kim, K.H. Baik, S.H. Yoo, C.G. Kim, Y.S. Kim, C.S. Kim, H.J. Kim, Y.E. Ihm, Phys. Status Solidi B 241 (2004) 1458.
[38] K.J. Lee, F.C. Yu, J.A. Kim, et al., Phys. Status Solidi B 241 (2004) 1525.
[39] I.T. Yoon, T.W. Kang, D.J. Kim, Mater. Sci. Eng. B 134 (2006) 49.